Journal of Sound and Vibration (1998) **212**(2), 253–264

EXACT SHARED MODAL FUNCTIONS AND FREQUENCIES FOR FIXED AND FREE ISOSPECTRAL MEMBRANE SHAPES FORMED FROM TRIANGLES

H. P. W. GOTTLIEB AND J. P. MCMANUS

Faculty of Science and Technology, Griffith University, Nathan, Brisbane, Qld 4111, *Australia*

(*Received* 23 *July* 1997, *and in final form* 27 *October* 1997)

For two different but isospectral polygonal membrane shapes (sharing the same complete vibration spectrum) formed from seven congruent elemental isosceles triangles, some exact shared frequencies and analytical modal function expressions which display the nodal curves are given explicitly. Both Dirichlet (fixed) and Neumann (free) boundary conditions are considered. Figures of the first few nodal patterns are drawn: they are quite distinctive and not all merely restricted to regular rectilinear sub-divisions. Computed modal function contour plots enable the overall sequential mode numbers to be assigned. The exact frequencies and sequential mode numbers for these analytical modes could be used as benchmarks in experimental investigations. The relevance for simply-supported polygonal plates is also discussed.

1. INTRODUCTION

A common problem in engineering and applied mathematics is the determination of the frequency spectrum of a vibrating membrane with some given shape and boundary condition. For the case of a uniform membrane, the partial differential equation to be solved is the Helmholtz equation

$$(\nabla^2 + k^2)u = 0, \tag{1}$$

where ∇^2 is the two-dimensional Laplacian ($\partial^2/\partial x^2 + \partial^2/\partial y^2$ in rectangular Cartesian co-ordinates) and the eigenvalue is k^2 with

$$k = 2\pi f/c, \tag{2}$$

where f is the characteristic frequency and c is the free wave speed. The shape together with the boundary condition determines the solution spectrum. The question arises: to what extent does the spectrum determine the shape?

Kac in the title of reference [1] asked "Can one hear the shape of a drum?". By utilizing the heat equation and its Green's function, he showed that a spectral function

$$E = \sum_N \exp(-k_N^2 s), \tag{3}$$

0022–460X/98/170253 + 12 $25.00/0/sv971436

for a shape with smooth boundary and Dirichlet (fixed) boundary condition

$$u = 0, \tag{4}$$

has the asymptotic expansion

$$E \sim A/(4\pi s) - L/[8(\pi s)^{1/2}] + (1 - h)/6 + O(s^{1/2}) \qquad \text{as} \qquad s \to 0. \tag{5}$$

Here, the membrane has area A, perimeter length L and h smooth holes; s is the expansion parameter. Subsequently, Stewartson and Waechter [2] showed that the terms in equation (5) after the first two could all be expressed in terms of the curvature of the boundary of the shape.

For Neumann (free) boundary condition

$$\partial u/\partial n = 0, \tag{6}$$

(where n denotes the normal to the boundary), Pleijel [3] and Sleeman [4] showed that the second, perimeter length, term in equation (5) changes sign.

For the situation such as that to be considered in this paper, of an irregular polygon, McKean and Singer [5] showed that the third (constant) term in equation (5) is replaced by a corner angle term. The spectral function expansion becomes

$$E = A/(4\pi s) \mp L/[8(\pi s)^{1/2}] + \sum_i (\pi^2 - \theta_i^2)/(24\pi\theta_i) + \cdots, \tag{7}$$

where the sum is taken over all the (possibly different) internal angles θ_i. In equation (7), the $-$ sign applies to Dirichlet boundary condition (4) and the $+$ sign to Neumann boundary condition (6).

Thus, the spectrum does determine certain geometrical features of the domain, such as area and perimeter, but it was an open question as to whether the spectrum uniquely determined the shape.

Counter examples for membranes were first discovered by Gordon *et al*. [6, 7], in the form of two distinct shapes made up of seven half-crosses in two different ways, colloquially referred to as "pound" and "yen" shapes. Popular accounts have been given by Cipra [8], Stewart [9] and Weidenmuller [10]. It is remarkable that membranes having these two different shapes nevertheless have exactly the same *complete* spectrum of characteristic frequencies. Such pairs of shapes are termed "isospectral". Thus, "one cannot hear the shape of a polygonal drum".

Subsequently, a pair of simpler isospectral shapes, each built up in a different way from seven "elemental" congruent isosceles right-angled triangles into an eight-sided polygon, was discovered (see e.g., Chapman [11]). These shapes are depicted in Figure 1. With regard to equation (7), they evidently possess the same area, perimeter length and internal angle set as each other. Equation (7) has been verified analytically in reference [12] for the elemental triangle of which these isospectral shapes are composed, by use of its explicitly known spectrum and the Poisson summation formula.

Sridhar and Kudrolli [13] adopted an experimental approach to verification of isospectrality, and measured some spectra of two very thin microwave cavities constructed with these isospectral shapes. Since the governing two-dimensional Helmholtz equation for the electromagnetic field (with Dirichlet boundary conditions) is of exactly the same form as equation (1), this represents a very effective utilization of physical analogies. Their results presented in reference [13] showed pairwise good agreement for the first 25 modes, and were reported as being typical of results up to the 54th mode. The authors there drew attention to the lack of analytical solutions and difficulties with possible numerical solutions.

Subsequently, Wu *et al*. [14] presented tabulated results of numerical computations for the first 25 modes, using extrapolated finite difference methods and mode-matching. They also showed some low-lying analytical mode functions. Then Driscoll [15, 16], using a modified finite element/domain decomposition method, gave much more accurate (to 12 digits) numerical results for the first 25 modes.

Chapman [11] proved that the two isospectral domains are also isospectral for the Neumann boundary condition. The main purpose of this paper is to exhibit further analytical nodes for the Dirichlet case and to present new exact analytical modes and frequencies with their nodal patterns for the Neumann case, and to identify their sequential mode numbers within the overall spectrum. These should be of use as calibrations in further investigations.

Some comments on polygonal plates are made in the Appendix.

2. ANALYTICAL MODES: FIXED (DIRICHLET) BOUNDARY CONDITION

General analytical solution for these shapes is not possible, so the modal frequencies and corresponding modal functions are not generally known [13]. However, techniques for writing down some explicit *analytical* functions and exact frequencies for certain modes of these types of compound shapes with fixed edges (Dirichlet boundary condition) were pursued some time ago by one of the authors, in reference [17].

A grid may be constructed consisting of squares of side length h (with origin at the corner of a square), and straight lines with slopes $\pm 45^\circ$ through the origin and other diagonal lines parallel to these separated (horizontally and vertically) by distances in multiples of $2h$. Part of such a grid is shown in Figure 1. Then, for any polygonal shape with edges restricted to lying on this grid, the following functions are solutions of equation (1) and satisfy the Dirichlet boundary condition (4) on the boundary lines:

$$u_{m,n}(x, y) = \sin(m\pi x/h)\sin(n\pi y/h) - \sin(n\pi x/h)\sin(m\pi y/h), \tag{8}$$

with $m < n$ being positive integers. That the boundary condition is satisfied on any line of the grid may be proved by noting, as in reference [17], that the expression on the right side of formula (8) can also be rewritten as

$$\sin[(m-n)\pi(x-y)/(2h)]\sin[(m+n)\pi(x+y)/(2h)]$$
$$-\sin[(m+n)\pi(x-y)/(2h)]\sin[(m-n)\pi(x+y)/(2h)]. \tag{9}$$

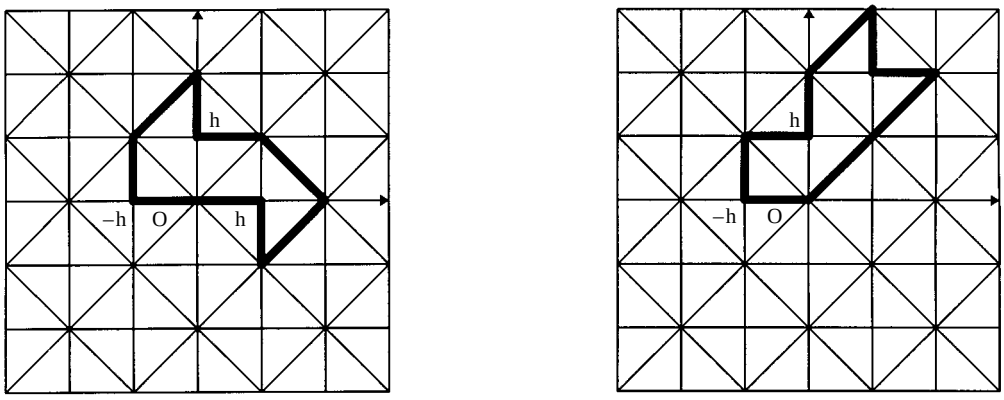

Figure 1. The two isospectral shapes superimposed on the grid with co-ordinate system (x-axis horizontal; y-axis vertical).

Equations (8) were also written down in reference [14] for the elemental sub-triangle, but it is important to note here that they actually refer to the whole shapes. That is, functions (8) constitute a set of *shared* mode functions for any shapes drawn on the grid, and hence in particular for both *entire* isospectral shapes, and are an analytical sub-set of all the modal functions.

The dimensionless squared frequency parameter is given for these modes exactly by

$$F^2 \equiv (h^2/\pi^2)k^2 = m^2 + n^2 \tag{10}$$

for this sub-sequence of the full spectrum. For given m and n, the nodal curves may be obtained mathematically from equations (8) after manipulations using appropriate trigonometrical identities.

The lowest member of the set (8), with $m = 1$, $n = 2$ ($F^2 = 5$), was given explicitly in reference [17] (cf. also reference [14]):

$$u_{1,2} = 4 \sin(\pi x/h) \sin(\pi y/h) \sin[\pi(x - y)/(2h)] \sin[\pi(x + y)/(2h)]. \tag{11}$$

With reference to the two isospectral shapes under consideration, its nodal lines are the internal straight lines dividing the shapes into the seven elementary triangular constituents. Some numerical computations have also been performed (see section 4), and this has been identified from the computed modal patterns as the 9th mode for both shapes, in agreement with reference [14]. The second member in this analytical subsequence has $m = 1$, $n = 3$ ($F^2 = 10$, i.e., exactly twice that of equation (11)), and the explicit mode function for either shape is given by

$$u_{1,3} = 4 \sin(\pi x/h) \sin(\pi y/h) \sin[\pi(x - y)/h] \sin[\pi(x + y)/h]. \tag{12}$$

The nodal pattern consists of 14 smaller congruent sub-triangular regions (i.e., the seven triangles mentioned above, halved). It was identified as the 21st mode, again in agreement with reference [14].

The next analytical mode corresponding to subdivisions into yet smaller triangles has $m = 2$, $n = 4$ ($F^2 = 20$), with 28 congruent sub-triangles, and is given by

$$u_{2,3} = 4 \sin(2\pi x/h) \sin(2\pi y/h) \sin[\pi(x - y)/h] \sin[\pi(x + y)/h]. \tag{13}$$

The computed modal pattern, discussed in section 4, revealed this as the 44th mode.

More interestingly, there are analytical modes, not depicted before, which are not simply sub-divisions into smaller sub-triangles. The third analytical mode in the above sequence, with $m = 2$, $n = 3$ ($F^2 = 13$), is the lowest such mode. Equation (8) becomes (cf. section 6 in reference [17]):

$$u_{2,3} = u_{1,2}[1 + 4 \cos(\pi x/h) \cos(\pi y/h)]. \tag{14}$$

As well as the nodal straight lines like the lowest analytical case $m = 1$, $n = 2$ (equation (11)), there are in this case also internal nodal curves corresponding to the bracketed expression in equation (14): these take the form of squared-off circles. There are 14 regions in these nodal patterns, but now seven are the quarter squared-off circles and seven are their complements from the elemental triangles, describable perhaps as "circus-tent" shapes (cf. also Barton [18, p. 273, Table IX]). Our computed mode function patterns identified this as the 27th mode.

One more such mode will be given here: for $m = 1$, $n = 4$ ($F^2 = 17$), it may be written as

$$u_{1,4} = 2u_{1,2}\{5 - 6[S_+^2 + S_-^2] + 8S_+^2 S_-^2\}, \tag{15a}$$

TABLE 1

Features of the first five analytical modes, equations (11–15), *for Dirichlet boundary condition* (4). *R = number of fundamental regions. N = sequential mode number*

m	n	F^2	R	N
1	2	5	7	9
1	3	10	14	21
2	3	13	14	27
1	4	17	14	38
2	4	20	28	44

where

$$S^2_{+,-} = \sin^2 [\pi(x \pm y)/(2h)]. \tag{15b}$$

The nodal pattern consists of the seven elemental triangles together with ovals or half-ovals lying across their diagonals, again giving 14 regions. This distinctive pattern enabled it to be identified from the computed modal patterns as the 38th mode.

Table 1 summarizes the features of these first five "analytical" modes. The nodal patterns for these modes, as obtained from the analytical expressions (11–15) above, are drawn for both shapes in Figure 2. Note that the boundaries of the shapes are also nodal lines, and, because of the form of equation (8), the extensions of any sides into the region must necessarily be nodal lines, in this case the seven elemental triangles. Whilst equations (11–15) are of course merely alternative forms of equation (8) obtained by using trigonometrical identities such as product and compound angle formulae, their forms exhibit the nodal lines and curves much more clearly.

3. ANALYTICAL MODES: FREE (NEUMANN) BOUNDARY CONDITIONS

For the case of free edges, with Neumann boundary condition

$$\mathrm{d}v/\mathrm{d}n = 0, \tag{16}$$

the appropriate modal functions are found to be

$$v_{m,n} = \cos(m\pi x/h)\cos(n\pi y/h) + \cos(n\pi x/h)\cos(m\pi y/h), \tag{17}$$

with $m \leqslant n$, with $m, n = 0, 1, 2, \ldots$ (except $m = n = 0$ which corresponds to a simple translation). Equation (1) is satisfied, again with eigenvalue given by equation (10).

The boundary condition (16) is satisfied on any line of the grid mentioned at the beginning of section 2. Clearly $\partial v/\partial x = 0$ on $x = Mh$ and $\partial v/\partial y = 0$ on $y = Nh$, where M and N are any integers. To demonstrate how the normal derivative is also zero on a diagonal line of the grid, it may be shown after some manipulation that

$$\begin{aligned}\partial v/\partial x + \partial v/\partial y = -(\pi/h)\{&(m+n)\sin[(m+n)(x+y)\pi/(2h)]\cos[(m-n)(x-y)\pi/(2h)] \\ &+(m-n)\sin[(m-n)(x+y)\pi/(2h)]\cos[(m+n)(x-y)\pi/(2h)]\}.\end{aligned} \tag{18}$$

If L is any integer, this clearly vanishes on the grid lines $x + y = 2Lh$, for which straight lines, the left side of equation (18) is the derivative in the direction perpendicular to these lines. Likewise, a similar expression is obtained for $\partial v/\partial x - \partial v/\partial y$, for which in the right side of equation (18) the relative $+$ and $-$ signs are interchanged within all the bracketed

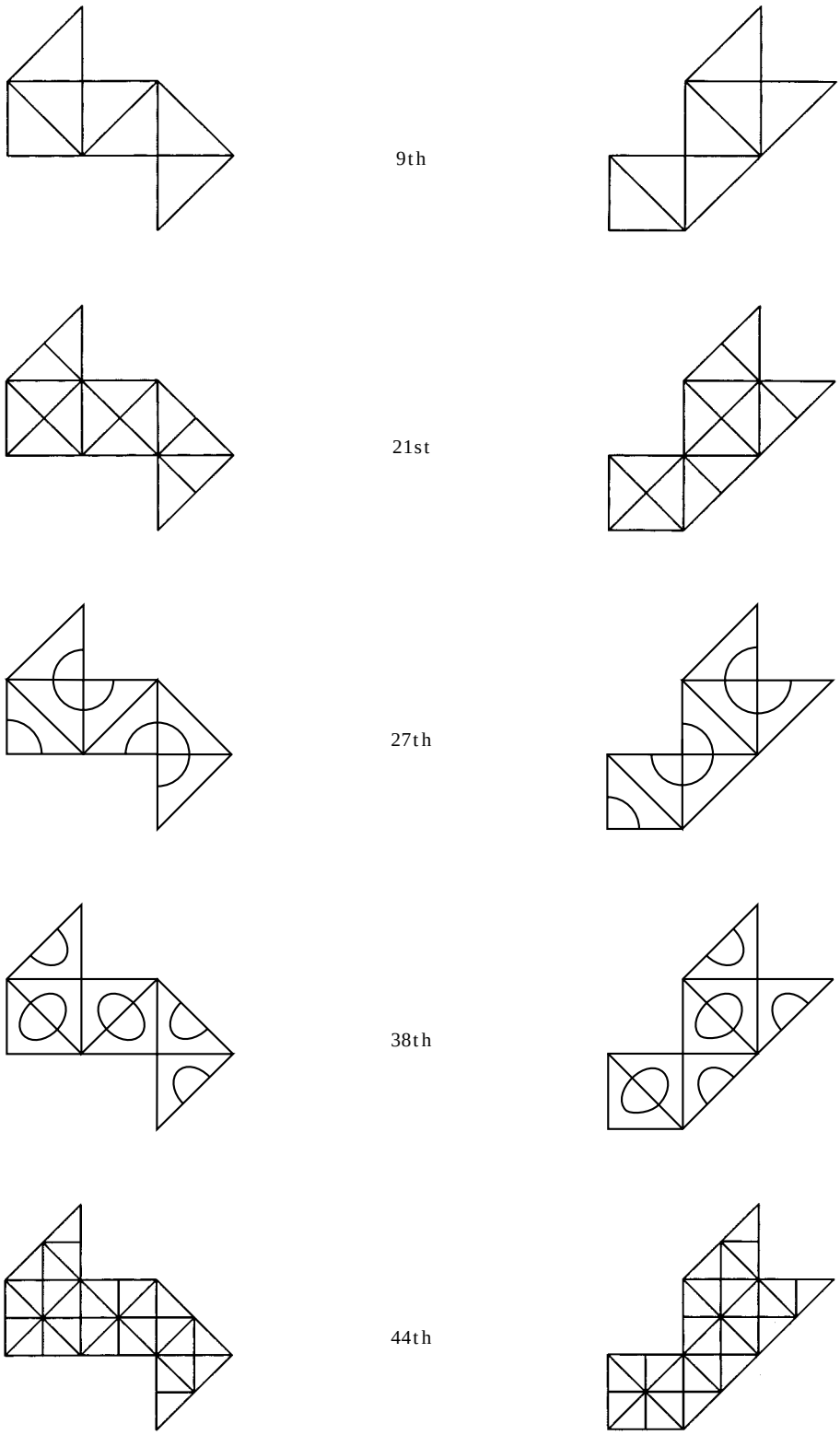

Figure 2. The nodal patterns for the first five analytical Dirichlet (fixed edge) modes given by equations (11–15). The overall sequential mode number is given. See also Table 1.

terms containing m and n, and containing x and y. If J is any integer, this vanishes on the grid lines $x - y = 2Jh$, to which this is the normal derivative for those lines.

Because zero integers are allowed, the characteristic frequencies are closer together than for the preceding Dirichlet case. Again the first five of these exact modes will be described now for this Neumann case, after rearrangements to simplify the analytical expressions.

For $m = 0$, $n = 1$ ($F^2 = 1$),

$$v_{0,1} = 2 \cos [\pi(x + y)/(2h) \cos [\pi(x - y)/(2h)]. \tag{19}$$

The nodal curves are all along some diagonal grid lines in this case. They are shown in Figure 3 (together with the next four analytical modes) for both of the isospectral shapes. Of course, now the edges of the shapes are *not* nodal lines, since they are in fact free. There are six regions for these patterns.

For $m = 1$, $n = 1$ ($F^2 = 2$),

$$v_{1,1} = 2 \cos (\pi x/h) \cos (\pi y/h). \tag{20}$$

The nodal lines are parallel to the x and y axes, and there are nine regions, as shown in Figure 3.

For $m = 0$, $n = 2$ ($F^2 = 4$),

$$v_{0,2} = 2 \cos [\pi(x + y)/h] \cos [\pi(x - y)/h]. \tag{21}$$

The nodal lines are in the diagonal directions, and there are 14 regions (see Figure 3).

The next mode with purely straight nodal lines, in this case horizontal and vertical, is the fifth in the analytical set, and has $m = 2$, $n = 2$ ($F^2 = 8$), with

$$v_{2,2} = 2 \cos (2\pi x/h) \cos (2\pi y/h). \tag{22}$$

It has 24 regions.

Of particular interest is the first analytical mode of the Neumann set which does not have solely straight lines. This is the fourth in the analytical set, with $m = 1$, $n = 2$ ($F^2 = 5$). Then, by some identities,

$$v_{1,2} = v_{0,1}\{2C_+^2 + 2C_-^2 - 3\}, \tag{23a}$$

where

$$C_{+,-}^2 = \cos^2 [\pi(x \pm y)/(2h)]. \tag{23b}$$

As well as the diagonal grid lines of the first analytical mode (equation (19)), there are also some nodal curves consisting of the curved boundaries of sectors of another kind of squared-off circle. Their "half-axis" (measured along the x or y directions) can easily be shown from equations (23) to be equal to 1/3. There are 12 regions for this mode.

Table 2 summarizes some features of these first five analytical modes for the Neumann case, and identifies their sequential mode numbers. In Figure 3 are drawn the corresponding nodal curves for both shapes, obtained from the manipulated expressions (19–23). The edges of these shapes, shown by a heavier line, are not nodal lines, being free for this boundary condition.

4. NUMERICAL COMPUTATIONS

Numerical computation of the eigenmodes enables the sequential mode number of the analytical modes to be found with respect to the whole sequence. The fixed (Dirichlet) modes will be dealt with first. Since accurate computational determinations of the eigenfrequencies have already been given by others [14–16], confirming the isospectrality

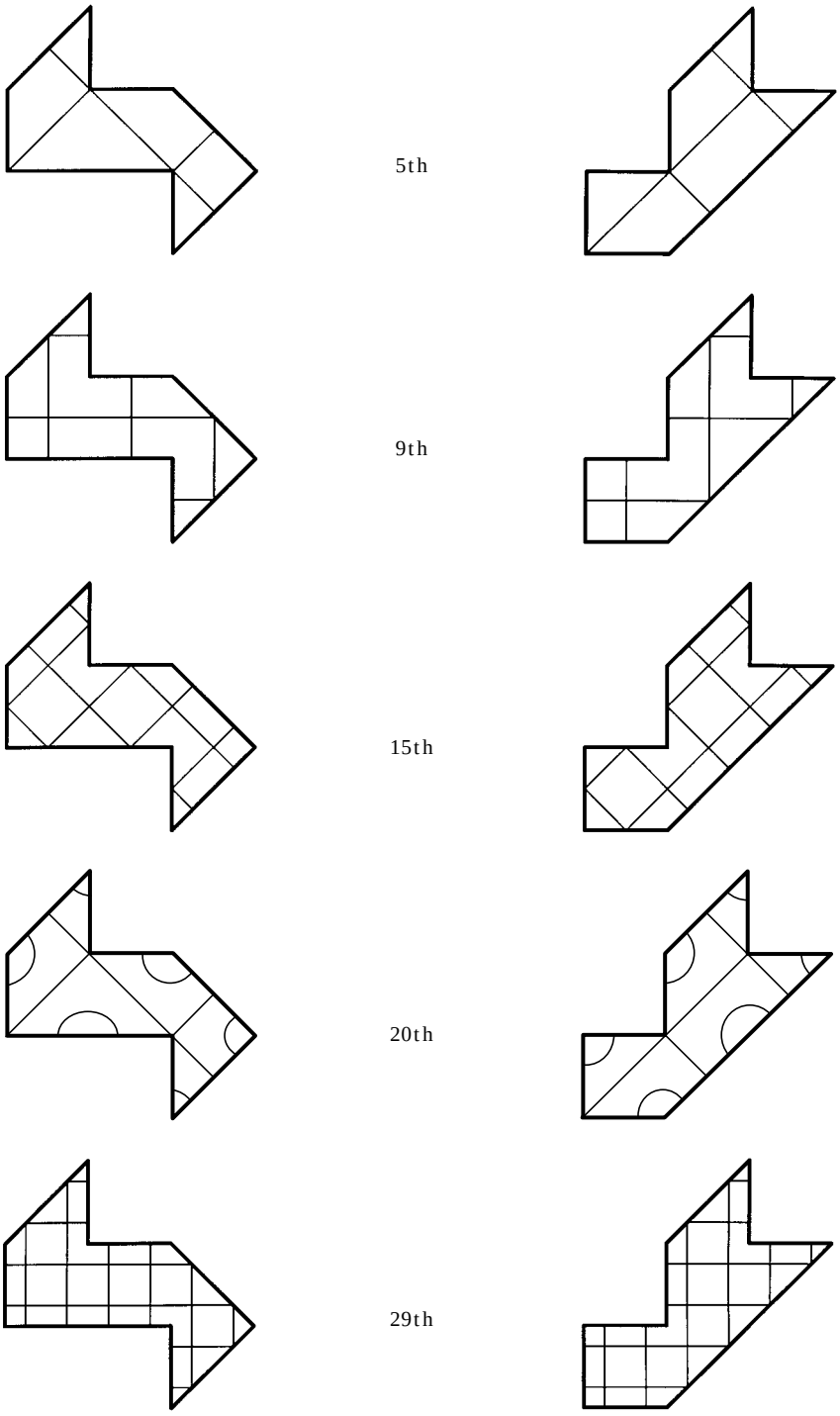

Figure 3. The nodal patterns for the first five analytical Neumann modes given by equations (19–23) (the edges are free, not nodal lines). The overall sequential positive-frequency mode number is given. See also Table 2.

numerically, the authors have not aimed for extreme accuracy, but rather on identification of the modal pattern from the given nodal curves for the analytical modes. Two rules [19] provide a useful qualitative check on the general appearance of any computed modal functions: (1) the number of fundamental regions (connected regions bounded by nodal curves, termed sub-domains in reference [19]) is less than or equal to the total sequential mode number; (2) nodal curves meet in an equiangular system.

Finite element methods and Matlab were used to compute the first 50 modal frequencies and functions for both shapes. The differences in computed k values for the two shapes were overall less than about 0·4%, and usually less than 0·1%, confirming isospectrality in this approximation. Our computed contour patterns agreed in appearance with those where available in published references [13, 10] (experimental) and [14–16] (computed).

Computations were also performed using the same procedure for the completely known analytical case of a 2×1 rectangle. These showed that (even though there were some small errors in eigenfrequencies) the degeneracies for this case were maintained, the sequential ordering of modes was correct, and identification of modes through contour plots was reliable.

The analytical nodal curves depicted in Figure 2 for the two isospectral shapes are so distinctive that they are easily identified amongst the computed modal patterns. Thus, their sequential order number (which was always the same for both shapes) was unambiguously assigned. The first 12 computed modes are available in reference [16], and computed modes corresponding to the lowest two analytical modes (9th and 21st in overall sequence) appear in reference [14]. Here, our computed modes are shown for the third and fifth analytical modes of the first shape, identified as the 27th and 44th modes in overall mode sequence, in Figure 4. Figure 5 shows our computed modes for both shapes for the fourth analytical mode, identified as the 38th sequential mode from our family of computed modes. The match with the corresponding analytical nodal curves drawn in Figure 2 is evident.

Further computations for the free (Neumann) modes enabled the sequential mode numbers of the first five analytical modes of the shapes, whose nodal curves are depicted in Figure 3, to be assigned. The results are summarized in Table 2.

5. CONCLUSION

Analytical modes such as those found here are characterized by their exactness and the distinctiveness of their nodal patterns. They may therefore be used as benchmarks, against

TABLE 2

Features of the first five analytical modes, equations (19–23), *for Neumann boundary condition* (16). *R = number of regions. N = sequential mode number* (*excluding the zero frequency mode*)

m	n	F^2	R	N
0	1	1	6	5
1	1	2	9	9
0	2	4	14	15
1	2	5	12	20
2	2	8	24	29

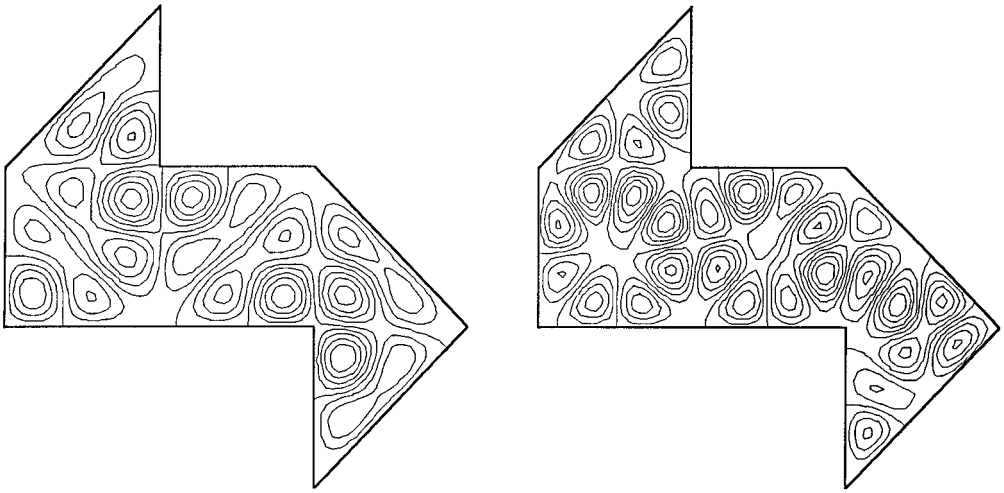

Figure 4. The computed modal function contours for the 27th and 44th Dirichlet modes of the first shape.

which other computational or experimental results can be calibrated once their mode patterns have been identified by comparisons with Figures 2 or 3. Even in experimental situations where only the characteristic frequencies (but not the harder-to-find mode functions) may have been measured, the sequential mode numbers should allow identification of these key modes from Tables 1 and 2.

Four such ratios may be utilized from the results in these tables. For example, for the Dirichlet case, the eigenvalue (or frequency-squared) ratios to the lowest analytical mode will be compared with the exact numbers 2:2·6:3·4:4. For the Neumann case, these ratios are 2:4:5:8. Furthermore, because of equation (10), comparisons may also be made between Dirichlet and Neumann modes by use of both Tables 1 and 2. For instance (if the same scale has been adhered to), the eigenvalue of the 9th Dirchlet mode should equal that of the 20th Neumann mode (case $m = 1$, $n = 2$).

Finally, on the more theoretical side, it is worth noting that Smilansky [20] pointed out that the question of uniqueness of shape corresponding to a given spectrum still remains

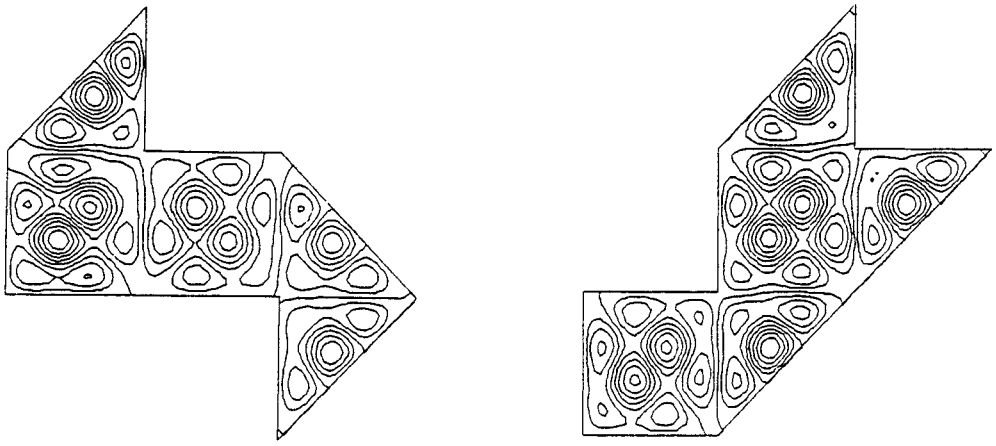

Figure 5. The computed modal function contours for the 38th Dirichlet mode for both shapes.

unanswered for shapes with smooth boundaries. Shapes such as those considered above and in references [6–11] not only have boundaries with corners but also have reflex angles. The uniqueness question for *convex* connected plane domains therefore still appears to be open.

ACKNOWLEDGMENTS

We are thankful to Professor S. Sridhar for supplying us with some higher-mode frequency measurements, and to Professor T. Driscoll for an earlier version of reference [15]. We also thank Dr A. J. O'Connor and Dr J. W. Lu for assistance.

REFERENCES

1. M. Kac 1966 *American Mathematical Monthly* **73**, 1–23. Can one hear the shape of a drum?
2. K. Stewartson and R. T. Waechter 1971 *Proceedings of the Cambridge Philosophical Society* **69**, 353–363. On hearing the shape of a drum: further results.
3. A. Pleijel 1953–1954 *Arkiv Matematik* **2**, 553–569. A study of certain Green's functions with applications in the theory of vibrating membranes.
4. B. D. Sleeman 1982 *IMA Journal of Applied Mathematics* **29**, 113–142. The inverse problem of acoustic scattering.
5. H. P. McKean and I. M. Singer 1967 *Journal of Differential Geometry* **1**, 43–69. Curvature and the eigenvalues of the Laplacian.
6. C. Gordon, D. L. Webb and S. Wolpert 1992 *Bulletin of the American Mathematical Society* **27**, 134–138. One cannot hear the shape of a drum.
7. C. Gordon, D. L. Webb and S. Wolpert 1992 *Inventiones Mathematicae* **110**, 1–22. Isospectral plane domains and surfaces via Riemannian orbifolds.
8. B. Cipra 1992 *Science* **225**, 1642–1643. You can't hear the shape of a drum.
9. I. Stewart 1992 *New Scientist* **1825**, 26–30. Beating out the shape of a drum.
10. H. Weidenmuller 1994 *Physics World* **7**, 22–23. Why different drums sound the same.
11. S. J. Chapman 1995 *American Mathematical Monthly* **102**, 124–138. Drums that sound the same.
12. H. P. W. Gottlieb 1988 *Journal of the Australian Mathematical Society Series B* **29**, 270–281. Eigenvalues of the Laplacian for rectilinear regions.
13. S. Sridhar and A. Kudrolli 1994 *Physical Review Letters* **72**, 2175–2178. Experiments on not "hearing the shape" of drums.
14. H. Wu, D. W. L. Sprung and J. Martorell 1995 *Physical Review E* **51**, 703–707. Numerical investigation of isospectral cavities built from triangles.
15. T. A. Driscoll 1997 *SIAM Review* **39**, 1–17. Eigenmodes of isospectral drums.
16. T. A. Driscoll 1996 *http://amath.colorado.edu/appm/faculty/tad/research/drums.html* Eigenmodes of isospectral drums.
17. H. P. W. Gottlieb 1985 *Journal of Sound and Vibration* **103**, 333–339. Exact vibration solutions for some irregularly shaped membranes and simply supported plates.
18. E. H. Barton 1919 *A Text-Book on Sound*. London: Macmillan.
19. R. Courant and D. Hilbert 1953/1989 *Methods of Mathematical Physics*, Vol. I. New York: Wiley. See pp. 395, 452.
20. U. Smilansky 1993 *Contemporary Physics* **34**, 297–302. On hearing the shape of a drum, and related problems.
21. A. W. Leissa 1969 *Vibration of Plates*, *NASA SP*-160. Washington: National Technical Information Service. See p. 237.
22. S. Timoshenko and S. Woinowsky-Krieger 1959 *Theory of Plates and Shells*. New York: McGraw-Hill; second edition. See p. 83.
23. H. D. Conway and K. A. Farnham 1965 *International Journal of Mechanical Sciences* **7**, 811–816. The free flexural vibrations of triangular, rhombic and parallelogram plates and some analogies.
24. R. D. Blevins 1984 *Formulas for Natural Frequency and Mode Shape*. Malabar: R. E. Krieger. See pp. 224–225, 239.

APPENDIX: CAN ONE HEAR THE SHAPE OF A GONG?

The characteristic frequencies and modal functions of a vibrating membrane with fixed, rectilinear edges and a plate of the same polygonal shape with simply-supported (hinged) edges are directly related through the membrane-plate analogy: the solutions have the same functional form, and the frequencies of the latter are proportional to the squares of the frequencies of the former. The plate results follow readily from the membrane problem [21, 22]. The membrane results follow from the plate problem in this configuration because the potentially extra frequencies from the higher (fourth) order plate equation are imaginary [23]. The analogy is therefore complete [24].

Thus, if two simply-supported plates take the shapes of the two distinct but isospectral polygonal fixed membranes depicted in Figure 1, that pair of plates will also be isospectral. Therefore, in the language of reference [1], "one cannot hear the shape of a polygonal gong": the frequency spectrum does not uniquely determine the shape. (For these purposes, the "gongs", with their required shapes and boundary condition, have rather more of a mathematical than a musical significance.)

We conclude by noting from the above that some isospectral membrane problems could therefore also be investigated numerically using engineering computer packages which handle plate vibrations.